

Absorption by Spinning Dust: a Contaminant for High-Redshift 21 cm Observations

B. T. Draine

Princeton University Observatory, Peyton Hall, Princeton, NJ 08544-1001, USA;
draine@astro.princeton.edu

Jordi Miralda-Escudé

Institut de Ciències del Cosmos, Universitat de Barcelona (IEEC-UB), 08028 Barcelona,
Catalonia, Spain; miralda@icc.ub.edu

ABSTRACT

Spinning dust grains in front of the bright Galactic synchrotron background can produce a weak absorption signal that could affect measurements of high-redshift 21 cm absorption. At frequencies near 80 MHz where the Experiment to Detect the Global EoR Signature (EDGES) experiment has reported 21 cm absorption at $z \approx 17$, absorption could be produced by interstellar nanoparticles with radii $a \approx 50 \text{ \AA}$ in the cold interstellar medium (ISM), with rotational temperature $T \approx 50 \text{ K}$. Atmospheric aerosols could contribute additional absorption. The strength of the absorption depends on the abundance of such grains and on their dipole moments, which are uncertain. The breadth of the absorption spectrum of spinning dust limits its possible impact on measurement of a relatively narrow 21 cm absorption feature.

Subject headings: atmospheric effects — atomic processes — cosmic background radiation — dust, extinction — radiation mechanisms: general — radio continuum: ISM

1. Introduction

Bowman et al. (2018) report a small decrease in the sky brightness in the 50–100 MHz region that has been interpreted as arising from 21 cm absorption of the cosmic microwave background (CMB) at redshift $z \sim 17$. The reported strength of the absorption signal, however, exceeds by a factor ~ 3 the largest model predictions based on an atomic intergalactic medium (IGM) that cools adiabatically after electron Thompson scattering can no longer keep the kinetic temperature coupled to the CMB temperature. This discrepancy has led to new physics being proposed, such as elastic scattering of dark matter by baryons or electrons that could lower the kinetic temperature of the baryons and possibly lead to a lowering of the spin temperature (Barkana 2018). This hypothesis, not motivated by theory or by independent observations, faces an additional difficulty: if the Lyman- α photons emitted by the first stars that are necessary to couple the spin and kinetic

temperature of the hydrogen gas through the Wouthuysen–Field effect are accompanied by as little as $\sim 1\%$ of their energy in X-ray emission or cosmic ray production, the resulting heating of the intergalactic gas would reduce the maximum strength of the absorption signal by a factor ~ 10 (Chen & Miralda-Escudé 2004; Hirata 2006). The first population of stars would therefore need to produce an anomalously low emission of X-rays and cosmic rays due to supernova remnants and X-ray binaries, compared to local starbursts (Oh 2001; Pacucci et al. 2014).

Observations of the CMB in this frequency range must contend with bright Galactic synchrotron emission with brightness temperature ranging over $1500 \lesssim T_B \lesssim 4000$ K at 78 MHz, so any frequency-dependent absorption (Galactic or telluric) interposed between us and the synchrotron emission will need to be recognized and, if significant, corrected for. For standard models, the expected signal due to 21 cm absorption at redshift $z \approx 17$ is at most $\Delta T_B \approx -0.2$ K (Zaldarriaga et al. 2004). Against a $T_B \sim 2000$ K background, an absorption optical depth $\tau \sim 10^{-4}$ would produce a signal of this magnitude.

Interstellar dust models (e.g., Draine & Li 2007) already include substantial populations of nanoparticles in order to explain the observed infrared emission, including strong emission features at 3.3, 6.2, 7.7, 8.6, 11.3, and $12.7\mu\text{m}$ attributed to polycyclic aromatic hydrocarbon (PAH) particles (Tielens 2008), as well as the “anomalous microwave emission” (Dickinson et al. 2018) that has been interpreted as rotational emission from $a \approx 5$ Å nanoparticles spinning at $\sim 15 - 60$ GHz (Draine & Lazarian 1998a). Here we explore the possibility that spinning interstellar dust grains with radii $a \approx 50$ Å could produce absorption in the 20 – 200 MHz frequency range. Rotational absorption by telluric aerosols could also affect ground-based observations. We find that absorption by interstellar dust or atmospheric aerosols is too broad to reproduce the signal reported by Bowman et al. (2018). However, this process (absorption of the bright Galactic synchrotron radiation by spinning dust) should be considered as a possible astrophysical “foreground” that could contaminate CMB observations in this frequency range.

2. Rotational Absorption by Spinning Dust

Consider grains of mass M and number density n_{gr} , in “Brownian rotation” at temperature T_{rot} , with an electric dipole moment μ_{\perp} perpendicular to the rotation axis. The volume-equivalent radius is $a = (3M/4\pi\rho)^{1/3}$, where ρ is the density. The moment of inertia is $I = \alpha(2/5)Ma^2$, where $\alpha = 1$ for a solid sphere. The total power emitted by one grain rotating at frequency ν is

$$P = \frac{2}{3} \frac{\mu_{\perp}^2}{c^3} (2\pi\nu)^4 . \quad (1)$$

The density of grains rotating at frequency ν within a range $d\nu$ is

$$f(\nu) d\nu = n_{\text{gr}} \frac{4\alpha^{3/2}}{\sqrt{\pi}\nu_T^3} e^{-\alpha(\nu/\nu_T)^2} \nu^2 d\nu . \quad (2)$$

The frequency ν_T is related to T_{rot} by

$$\nu_T \equiv \left(\frac{15k_{\text{B}}T_{\text{rot}}}{16\pi^3\rho a^5} \right)^{1/2} = 58 \left(\frac{T_{\text{rot}}}{50 \text{ K}} \right)^{1/2} \left(\frac{2 \text{ g cm}^{-3}}{\rho} \right)^{1/2} \left(\frac{50 \text{ \AA}}{a} \right)^{5/2} \text{ MHz} . \quad (3)$$

The power radiated in frequency interval $d\nu$ per unit volume and steradian is then

$$j_{\nu}d\nu = \frac{n_{\text{gr}}}{4\pi} \frac{2}{3} \frac{\mu_{\perp}^2}{c^3} (2\pi\nu)^4 \frac{4\alpha^{3/2}}{\sqrt{\pi\nu_T^3}} e^{-\alpha(\nu/\nu_T)^2} \nu^2 d\nu . \quad (4)$$

The effective absorption cross section (i.e., true absorption minus stimulated emission) is obtained from Kirchoff's law (in the Rayleigh-Jeans limit $B_{\nu}(T_{\text{rot}}) = 2kT_{\text{rot}}\nu^2/c^2$),

$$n_{\text{gr}}C_{\text{abs}}(\nu) = \frac{j_{\nu}}{B_{\nu}(T_{\text{rot}})} \quad (5)$$

$$= n_{\text{gr}} \frac{2^{10}\pi^7}{45\sqrt{15}} \frac{\mu_{\perp}^2}{c} \frac{\rho^{3/2}a^{15/2}}{(k_{\text{B}}T_{\text{rot}})^{5/2}} \alpha^{3/2} \nu^4 e^{-\alpha(\nu/\nu_T)^2} . \quad (6)$$

This cross section $C_{\text{abs}}(\nu)$ peaks at a frequency

$$\nu_{\text{peak}} = \sqrt{\frac{2}{\alpha}} \nu_T = \frac{82}{\sqrt{\alpha}} \left(\frac{T_{\text{rot}}}{50 \text{ K}} \right)^{1/2} \left(\frac{2 \text{ g cm}^{-3}}{\rho} \right)^{1/2} \left(\frac{50 \text{ \AA}}{a} \right)^{5/2} \text{ MHz} . \quad (7)$$

The $\nu^4 e^{-\alpha(\nu/\nu_T)^2}$ dependence of the opacity in Eq. (6) is for the thermal distribution of Eq. (2), exact for spheres. The cutoff frequency is $\nu_T \propto \sqrt{T_{\text{rot}}/I}$, where I is the moment of inertia. For more realistic grain shapes, the moment of inertia tensor has eigenvalues $I_1 > I_2 > I_3$, and the distribution of rotation frequencies is complicated. Even a single grain with fixed angular momentum J and fixed rotational kinetic energy E_{rot} has multiple frequencies characterizing its tumbling (see, e.g., Weingartner & Draine 2003; Hoang et al. 2011). The rotational dynamics are further complicated if the grain's vibrational temperature $T_{\text{vib}} < T_{\text{rot}}$, as is generally the case for interstellar grains: the particle then tends to align its principal axis with largest moment of inertia with the angular momentum vector.

Define $\alpha_j \equiv I_j/(\frac{2}{5}Ma^2)$. For example, an ellipsoid with axial ratios 1: $\sqrt{2}$:2 has $(\alpha_1, \alpha_2, \alpha_3) = (1.5, 1.25, 0.75)$. An exact description of rotation for triaxial shapes is beyond the scope of the present work, but a simple approximation is to average over thermal distributions for spheres for the three α_j :

$$f(\nu)d\nu \approx n_{\text{gr}} \frac{4}{\sqrt{\pi}} \nu^2 d\nu \times \frac{1}{3} \sum_{j=1}^3 \frac{\alpha_j^{3/2}}{\nu_T^3} e^{-\alpha_j(\nu/\nu_T)^2} \quad (8)$$

$$n_{\text{gr}}C_{\text{abs}} \approx n_{\text{gr}} \frac{2^{10}\pi^7}{45\sqrt{15}} \frac{\mu_{\perp}^2}{c} \frac{\rho^{3/2}a^{15/2}}{(kT_{\text{rot}})^{5/2}} \nu^4 \times \frac{1}{3} \sum_{j=1}^3 \alpha_j^{3/2} e^{-\alpha_j(\nu/\nu_T)^2} . \quad (9)$$

The actual distribution for a triaxial body in thermal equilibrium is expected to be intermediate between Eq. (8) and the simple thermal distribution (2) for a single $\bar{\alpha} = (\alpha_1 + \alpha_2 + \alpha_3)/3$. We will compare these below.

3. Nanoparticle Abundances

The composition and size distribution of interstellar grains remain uncertain. Models to reproduce the optical and UV extinction require a size distribution with most of the grain mass concentrated in the 0.05–0.5 μm size range. However, a substantial additional population of smaller grains is required to account for the ultraviolet extinction. A significant fraction of the smallest particles, containing as few as ~ 50 atoms, must be composed of polycyclic aromatic hydrocarbons (PAHs) in order to account for the observed strong infrared emission bands at 3.3, 6.2, 7.7, 8.6, 11.3, and 12.7 μm . In the model of Draine & Li (2007), the PAH nanoparticles are concentrated in two populations – one with the mass distribution peaking near 6 Å, containing $\sim 15\%$ of the interstellar carbon, and one peaking near 50 Å, containing $\sim 5\%$ of the interstellar carbon. The latter population was invoked to account for observed 24 μm continuum emission from the ISM of spiral galaxies.

If composed primarily of carbon (perhaps PAHs), these particles would have a mean density $\rho \approx 2 \text{ g cm}^{-3}$, and a number of atoms $N \approx 5 \times 10^4 (a/50 \text{ Å})^3$. Nanoparticles with other compositions, such as silicate, may also be numerous without violating observational constraints (Hensley & Draine 2017a). A substantial fraction of the iron in the ISM could be in the form of metallic Fe nanoparticles (Hensley & Draine 2017b), iron oxides, or other material.

The interstellar grain size distribution is the result of a balance between grain growth (by accretion and coagulation), and grain destruction (by vaporization and fragmentation in grain-grain collisions, sputtering in hot gas, and photodestruction of the smallest grains). It is at least conceivable that the larger $\gtrsim 0.1\mu\text{m}$ interstellar grains might consist of domains containing $\sim 10^4 - 10^5$ atoms, with shattering producing a fragmentation spectrum peaking in this size range. As noted above, models aiming to reproduce the infrared emission (Draine & Li 2007) specifically included a component peaking at this size. A peak in the size distribution would result in a peak in the spinning dust absorption spectrum.

4. Nanoparticle Dipole Moments

If the rotation axis is uncorrelated with the direction of the electric dipole moment, then

$$\langle \mu_{\perp}^2 \rangle = \frac{2}{3} \mu^2, \quad (10)$$

where μ is the total electric dipole moment of the grain. We will be primarily interested in nanoparticles with radii $a \approx 50 \text{ Å}$. Several different effects may contribute to μ .

Amorphous materials: an amorphous material can be thought of as a random aggregation of structural units with no long-range order. A nanoparticle of amorphous composition might then have an electric dipole moment $\mu \approx \mu_{\text{unit}} \times \sqrt{N/N_{\text{unit}}}$ where N_{unit} is the number of atoms in one structural unit, and μ_{unit} is the typical dipole moment of a structural unit. The aliphatic C–H bond

has a dipole moment 0.3 D (D \equiv Debye $\equiv 10^{-18}$ esu cm), the Si–H bond has a dipole moment 1.0 D (Speight 2005), and the Si–O bond has dipole moment 0.95 D (Freiser et al. 1953). For materials with polar structural units, values of $\mu_{\text{unit}}/\sqrt{N_{\text{unit}}} \approx$ few Debye are plausible, thus for $N \approx 5 \times 10^4$ one might expect $\mu \approx 200 \times \text{few D}$.

Inhomogeneous nanoparticles: the nanoparticle may be an aggregation of different materials with different work functions (i.e., different Fermi levels). If the materials are metals, then electrons will flow to develop a “contact potential” between the different components. To illustrate this, suppose that the nanoparticle consisted of two conducting hemispheres with a small gap δ separating the hemispheres. To produce a potential difference $\Delta V_{\text{contact}}$ between the hemispheres, the electric field in the gap would be $E_{\text{gap}} = \Delta V_{\text{contact}}/\delta$, with a charge $\pm Q$ on each side of the gap, with $Q = E_{\text{gap}} \times (\pi a^2/4\pi)$. The electric dipole moment of this “double layer” is

$$\mu = Q\delta = (\Delta V_{\text{contact}}) \frac{a^2}{4} = 210 \left(\frac{\Delta V_{\text{contact}}}{\text{Volt}} \right) \left(\frac{a}{50 \text{ \AA}} \right)^2 \text{ D} , \quad (11)$$

independent of δ . Contact potentials $\Delta V_{\text{contact}} \approx 1\text{Volt}$ are plausible. Thus, one might expect $\mu \approx 200 \text{ D}$ from this effect.

Ionized nanoparticles: capture of electrons and photoionization can result in negatively or positively charged nanoparticles. If photoionization is faster than electron capture for a neutral particle, then it will generally be found positively charged, with a net potential U , and a net charge

$$Z = \frac{Ua}{e} = 3.5 \left(\frac{U}{\text{Volt}} \right) \left(\frac{a}{50 \text{ \AA}} \right) . \quad (12)$$

If the grain is metallic, the surface will be an equipotential. Purcell (1975) noted that for moderately irregular isopotential surfaces, the center of charge deviates from the centroid by perhaps $\sim 2\%$ of the characteristic radius, in which case the dipole moment would be only

$$\mu \approx 0.02Zea \approx 16 \left(\frac{U}{\text{Volt}} \right) \left(\frac{a}{50 \text{ \AA}} \right) \text{ D} . \quad (13)$$

On the other hand, if the material is an insulator, the excess charge may be localized at a small number of points on the surface. A single charge e separated from the center of mass by a distance 5×10^{-7} cm corresponds to $\mu = 240 \text{ D}$. This dipole moment will, however, be partially compensated by polarization of the grain material, but the resulting net dipole moment could plausibly be $\sim 100 \text{ D}$ for a grain with charge $Z = \pm 1$. Grains with two or three charged sites (which might include both positive and negative charges) could have larger μ .

Ferroelectric inclusions: Some materials become spontaneously electrically polarized when cooled below a critical temperature, a phenomenon referred to as ferroelectricity (see, e.g., Xu 1991). Ferroelectric materials are used as piezoelectrics, computer memory, and liquid crystal displays. Technologically important materials usually contain cosmically scarce elements such as Ti or Ba (e.g., BaTiO_3). However, HCl, KNO_3 and NH_4NO_3 are also ferroelectrics, so one should

consider the possibility that interstellar nanoparticles may contain ferroelectric inclusions. A low-temperature ferroelectric phase of H₂O ice has also been reported (Fukazawa et al. 2006). With dipole moments per atom reaching values of ~ 1 D, if a fraction f_{fe} of a nanoparticle consisted of a ferroelectric domain, the net dipole moment could reach $\mu \sim f_{\text{fe}}N$ D, or $\sim 10^3$ D for $f_{\text{fe}} = 2\%$ and $N = 5 \times 10^4$.

Polarized ice mantles: ices deposited on grains can also be spontaneously polarized (Field et al. 2013; Plekan et al. 2017) by either the substrate itself or the electric field if the grain is charged. This polarization can extend through hundreds of monolayers, but the observed net polarization per dipole is only a few percent of the intrinsic dipole moment per molecule. If one region on the surface of a nanoparticle had $\sim 10^3$ molecules deposited in polarized form, this domain might contribute an electric dipole moment of $\sim 10^2$ D.

Ferromagnetism: interstellar grains may contain ferrimagnetic or ferromagnetic material giving the nanoparticle a permanent magnetic dipole moment (see, e.g., Draine & Hensley 2013, and references therein). The rotational emissivity is still given by Eq. (4), but with μ_{\perp}^2 replaced by $(\mu_{e,\perp}^2 + \mu_{m,\perp}^2)$ where $\mu_{e,\perp}$ and $\mu_{m,\perp}$ are the electric and magnetic dipole moments perpendicular to the rotation axis. If the grain contains N_{Fe} atoms in a single ferromagnetic domain, then $\mu_m = 200(N_{\text{Fe}}/10^4)$ D, assuming $2.2\mu_B$ per Fe atom as in metallic Fe (Bohr magneton $\mu_B = 0.0093$ D).

Each of the above effects leads to dipole moments that might be as large as $|\mu| \approx$ few hundred Debye. As they will act more or less independently, overall dipole moments μ as large as $\sim 10^3$ D are not implausible. Given the uncertainties in the relevant physics, dipole moments as large as ~ 2000 D for $a = 50$ Å cannot be ruled out at this time.

5. Rotational Excitation and Damping

A number of processes contribute to rotational excitation and damping of interstellar nanoparticles. Draine & Lazarian (1998b, see Figs. 4 and 5) compared the importance of different processes as a function of grain size. For $a \approx 50$ Å and the μ values estimated above, one can show that damping resulting from electric dipole radiation, and excitation of rotation by energy absorbed from the synchrotron background, have negligible effects on the grain rotation. For nanoparticles with $a \approx 50$ Å the rotational distribution is expected to be approximately thermal, with $T_{\text{rot}} \approx 50$ K. For grains of this size, the rotational temperature tends to be lower than the kinetic temperature of the gas because of damping by infrared emission (Hoang et al. 2011; Draine & Hensley 2016).

6. Discussion

With the absorption cross section from Eq. (6), dust in the ISM would contribute an optical depth

$$\tau_{\text{rot}} = N_{\text{H}} \frac{n_{\text{gr}}}{n_{\text{H}}} C_{\text{abs}}(\nu) = N_{\text{H}} X_{\text{gr}} \frac{2^8 \pi^6}{15 \sqrt{15}} \frac{\mu_{\perp}^2 m_{\text{H}}}{c} \frac{\rho^{1/2} a^{9/2}}{(k_{\text{B}} T_{\text{rot}})^{5/2}} \nu^4 \alpha^{3/2} e^{-\alpha(\nu/\nu_T)^2} \quad (14)$$

$$= 5.96 \times 10^{-4} \left(\frac{N_{\text{H}}}{10^{21} \text{ cm}^{-2}} \right) \left(\frac{X_{\text{gr}}}{4 \times 10^{-4}} \right) \left(\frac{\mu}{2000 \text{ D}} \right)^2 \left(\frac{a}{50 \text{ \AA}} \right)^{9/2} \times \left(\frac{\rho}{2 \text{ g cm}^{-3}} \right)^{1/2} \left(\frac{50 \text{ K}}{T_{\text{rot}}} \right)^{5/2} \left(\frac{\nu}{100 \text{ MHz}} \right)^4 \alpha^{3/2} e^{-\alpha(\nu/\nu_T)^2}, \quad (15)$$

where we have set $\mu_{\perp}^2 = (2/3)\mu^2$,

$$X_{\text{gr}} \equiv \frac{n_{\text{gr}} 4\pi\rho a^3}{n_{\text{H}} 3m_{\text{H}}} \quad (16)$$

is the mass in the dust component relative to the mass of H in the ISM, m_{H} is the mass of the hydrogen atom, and ν_T is given by Eq. (3). For all grains in the ISM we have $\sum X_{\text{gr}} \approx 0.010$ (Draine 2011). If T_{rot} is less than the brightness temperature of the synchrotron background, the dust will appear in absorption.

For $N_{\text{H}} = 10^{21} \text{ cm}^{-2}$ the “vibrational” modes of dust grains are estimated to contribute $\tau \approx 1 \times 10^{-7} (\nu/100 \text{ GHz})^{1.7}$ at $\nu < 400 \text{ GHz}$ (Li & Draine 2001), extrapolating to $\tau \approx 10^{-12}$ at 100 MHz. Absorption by aligned spins in ferromagnetic grains (Draine & Hensley 2013) could increase this to $\sim 10^{-9}$ if most of the Fe is in metallic form, but this is still completely negligible.

From Eq. (15) we see that for $\mu \lesssim 100 \text{ D}$, spinning dust absorption would contribute negligibly to the signal reported by Bowman et al. (2018). However, if we instead take $\mu = 2000 \text{ D}$ and $a \approx 50 \text{ \AA}$, we have $\tau_{\text{rot}} \approx 2 \times 10^{-5}$ near 80 MHz (see Fig. 1a). Such absorption would produce a signal comparable to the predicted cosmological signal for realistic scenarios where the harmonic-mean spin temperature is intermediate between the CMB temperature and the kinetic temperature of the H I.

If the grains have a single size, the absorption will be peaked as seen in Figure 1a, with $\Delta\nu_{\text{FWHM}} = 0.82\nu_{\text{peak}}$. For the more realistic case of a size distribution, the absorption feature will be broadened, with $\Delta\nu_{\text{FWHM}}/\nu_{\text{peak}} > 0.82$.

Suppose that a column density $N_{\text{H}} = 10^{21} \text{ cm}^{-2}$ of diffuse ISM is situated in front of a background with brightness temperature

$$T_{\text{back}} = 2.73 \text{ K} + T_{\text{sync}} \quad (17)$$

where

$$T_{\text{sync}} = 900 \left(\frac{\nu}{100 \text{ MHz}} \right)^{-2.43} \text{ K} \quad (18)$$

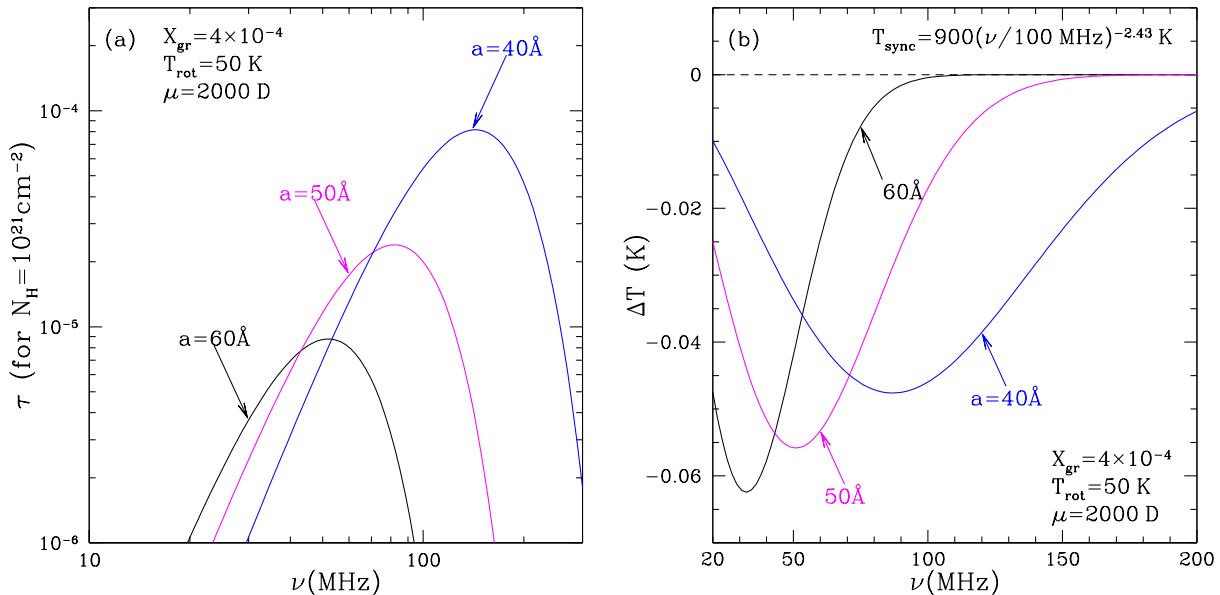


Fig. 1.— (a) Optical depth produced by nanoparticles in a column $N_H = 10^{21} \text{ cm}^{-2}$ of CNM. Each curve is for nanoparticles of the indicated size with total mass relative to H $X_{\text{gr}} = 4 \times 10^{-4}$ and $\mu = 2000 \text{ D}$. (b) Absorption signal for assumed synchrotron background of Eq. (18).

approximates the synchrotron brightness temperature reported by Bowman et al. (2018). The reduction in brightness temperature is

$$\Delta T = (T_{\text{rot}} - T_{\text{back}}) (1 - e^{-\tau}) \approx (T_{\text{rot}} - T_{\text{back}}) \tau . \quad (19)$$

Figure 1b shows the decrease in sky brightness for three grain sizes. For $T_{\text{rot}} < 100 \text{ K}$, spinning dust would appear in absorption for $\nu \lesssim 200 \text{ MHz}$.

The effect of grain nonsphericity is illustrated in Figure 2, comparing absorption by ellipsoids with axial ratios $1:\sqrt{2}:2$, estimated from Eq. (8), to the absorption for spheres of the same mass and $\bar{\alpha} = 7/6$. Triaxiality does broaden the absorption profile, but the effects are small compared to the effect of a distribution of grain sizes.

The absorption produced even by single-sized grains is significantly broader than the absorption profile reported by Bowman et al. (2018). However, adding a dust absorption component to the background model can provide more flexibility for fitting the observed shape of the total spectrum and could reduce the required narrower component that is attributed to high-redshift 21 cm absorption.

In addition to interstellar nanoparticles, atmospheric aerosols could also affect ground-based observations. Let Σ be the mass surface density in aerosol particles of radius a along the path

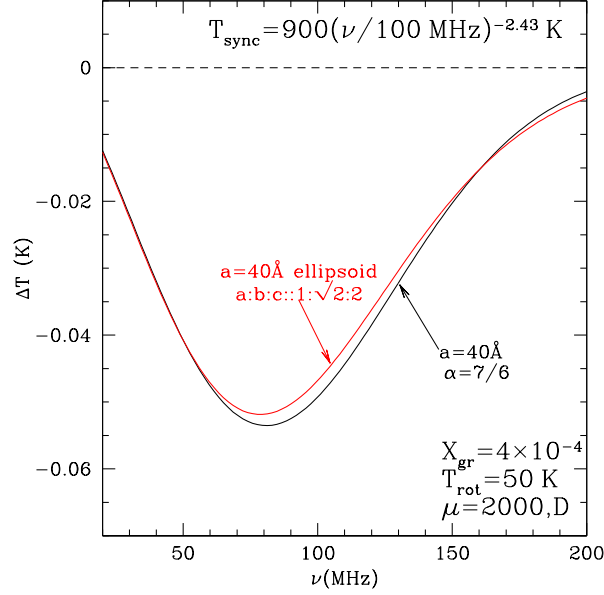


Fig. 2.— Absorption by ellipsoidal grains with volume-equivalent radius $a = 40 \text{ \AA}$, estimated from Eq. (8), compared to a $a = 40 \text{ \AA}$ spheres and $\bar{\alpha} = 7/6$.

through the atmosphere. The optical depth is

$$\tau_{\text{rot}} = \frac{2\mu^2\Sigma}{3\rho a^3 c} \left(\frac{15}{\rho a^5 k_B T_{\text{rot}}} \right)^{1/2} \left(\frac{\nu}{\nu_T} \right)^4 e^{-(\nu/\nu_T)^2} \quad (20)$$

$$= 1.2 \times 10^{-4} \left(\frac{\Sigma}{\mu\text{g cm}^{-2}} \right) \left(\frac{\mu}{10^4 \text{ D}} \right)^2 \left(\frac{70 \text{ \AA}}{a} \right)^{11/2} \left(\frac{\nu}{\nu_T} \right)^4 e^{-(\nu/\nu_T)^2}, \quad (21)$$

where $T_{\text{rot}} \approx 250 \text{ K}$ and ν_T is given by Eq. (3). For the synchrotron brightness of Eq. (18), aerosols would appear in absorption for $\nu \lesssim 150 \text{ MHz}$.

Measurements of atmospheric aerosols in Finnish forests (Dal Maso et al. 2005) show a peak near $a \approx 30 \text{ \AA}$, and a second peak near 200 \AA , but little appears to be known about the abundances or compositions of very small aerosols at other locations or altitudes. Nanoparticles with sizes $a \lesssim 100 \text{ \AA}$ are difficult to collect and identify. Because they are inefficient at scattering optical light, they do not appear directly as noctilucent clouds. In the upper stratosphere, such particles are likely to be primarily solids of interplanetary origin (Flynn 1994), or condensates from material ablated from meteors (Hunten et al. 1980). However, Hunten et al. (1980) estimate concentrations of only $\sim 10^3 \text{ cm}^{-3}$, or $\Sigma \sim 10^{-3} \mu\text{g cm}^{-2}$, too small to be of interest here.

In the lower atmosphere, nanoparticles include water droplets and ice crystals, and products of both natural and anthropogenic combustion. Droplets will spin like solid spheres, but will presumably lack the large dipole moments required to produce significant rotational absorption.

7. Summary

Spinning nanoparticles in the ISM with radii $\sim 50 \text{ \AA}$ can absorb radiation from the bright synchrotron background, producing variations in the brightness of the radio sky near 80 MHz that might be misinterpreted as arising from 21 cm absorption of the CMB at high redshift.

Because the spinning dust absorption would be correlated with other dust tracers (e.g., FIR emission from the larger grains), such absorption could presumably be recognized and corrected for in maps by spatial correlation with other known astrophysical foregrounds (e.g., emission from dust at submm and microwave frequencies).

If atmospheric aerosols with radii $\sim 70 \text{ \AA}$ are abundant and have large dipole moments, they could also contribute absorption below $\sim 150 \text{ MHz}$. Such absorption would of course be recognizable by its time dependence.

This research was supported in part by NSF grant AST-1408723, and in part by Spanish grants AYA2015-71091-P and MDM-2014-0369.

REFERENCES

- Barkana, R. 2018, *Nature*, 555, 71
- Bowman, J. D., Rogers, A. E. E., Monsalve, R. A., Mozdzen, T. J., & Mahesh, N. 2018, *Nature*, 555, 67
- Chen, X., & Miralda-Escudé, J. 2004, *ApJ*, 602, 1
- Dal Maso, M., Kulmala, M., Riipinen, I., et al. 2005, *Boreal Environment Research*, 10, 323
- Dickinson, C., Ali-Haïmoud, Y., Barr, A., et al. 2018, *New A Rev.*, 80, 1
- Draine, B. T. 2011, *Physics of the Interstellar and Intergalactic Medium* (Princeton, NJ: Princeton Univ. Press)
- Draine, B. T., & Hensley, B. 2013, *ApJ*, 765, 159
- Draine, B. T., & Hensley, B. S. 2016, *ApJ*, 831, 59
- Draine, B. T., & Lazarian, A. 1998a, *ApJ*, 494, L19
- Draine, B. T., & Lazarian, A. 1998b, *ApJ*, 508, 157
- Draine, B. T., & Li, A. 2007, *ApJ*, 657, 810
- Field, D., Plekan, O., Cassidy, A., et al. 2013, *International Reviews in Physical Chemistry*, 32, 345

- Flynn, G. J. 1994, *Planet. Space Sci.*, 42, 1151
- Freiser, H., Eagle, M. V., & Speier, J. 1953, *J. American Chemical Society*, 75, 2824
- Fukazawa, H., Hoshikawa, A., Ishii, Y., Chakoumakos, B. C., & Fernandez-Baca, J. A. 2006, *ApJ*, 652, L57
- Hensley, B. S., & Draine, B. T. 2017a, *ApJ*, 836, 179
- Hensley, B. S., & Draine, B. T. 2017b, *ApJ*, 834, 134
- Hirata, C. M. 2006, *MNRAS*, 367, 259
- Hoang, T., Lazarian, A., & Draine, B. T. 2011, *ApJ*, 741, 87
- Hunten, D. M., Turco, R. P., & Toon, O. B. 1980, *Journal of Atmospheric Sciences*, 37, 1342
- Li, A., & Draine, B. T. 2001, *ApJ*, 554, 778
- Oh, S. P. 2001, *ApJ*, 553, 499
- Pacucci, F., Mesinger, A., Mineo, S., & Ferrara, A. 2014, *MNRAS*, 443, 678
- Plekan, O., Rosu-Finsen, A., Cassidy, A. M., et al. 2017, *European Physical Journal D*, 71, 162
- Purcell, E. M. 1975, in *The Dusty Universe*, ed. G. B. Field & A. G. W. Cameron (New York: Neale Watson Academic), 155
- Speight, J. 2005, *Lange’s Handbook of Chemistry, Sixteenth Edition* (New York: McGraw-Hill Education)
- Tielens, A. G. G. M. 2008, *ARA&A*, 46, 289
- Weingartner, J. C., & Draine, B. T. 2003, *ApJ*, 589, 289
- Xu, Y. 1991, *Ferroelectric Materials and Their Applications* (New York: North-Holland)
- Zaldarriaga, M., Furlanetto, S. R., & Hernquist, L. 2004, *ApJ*, 608, 622